Available online at www.sciencedirect.com
ScienceDirect
Journal of the European Ceramic Society 30 (2010) 2749–2755
www.elsevier.com/locate/jeurceramsoc

Effect of microscale shear stresses on the martensitic phase transformation of nanocrystalline tetragonal zirconia powders

Mette Skovgaard [a,c], Anwar Ahniyaz [b,*], Bent F. Sørensen [c], Kristoffer Almdal [d], Alexander van Lelieveld [e]

[a] *DentoFit A/S, Frederiksborgvej 399, DK-4000 Roskilde, Denmark*
[b] *YKI, Institute for Surface Chemistry, 11486 Stockholm, Sweden*
[c] *Materials Research Division, Risø National Laboratory for Sustainable Energy, Technical University of Denmark, DK-4000 Roskilde, Denmark*
[d] *Department of Micro- and Nanotechnology, Technical University of Denmark, DK-4000 Roskilde, Denmark*
[e] *Aneedle, Engelstedsgade 322, DK-2100 Copenhagen East, Denmark*

Received 11 April 2010; accepted 20 May 2010

Abstract

For the first time, the effect of microscale shear stress induced by both mechanical compression and ball-milling on the phase stability of nanocrystalline tetragonal zirconia (t-ZrO_2) powders was studied in water free, inert atmosphere. It was found that nanocrystalline t-ZrO_2 powders are extremely sensitive to both macroscopic uniaxial compressive strain and ball-milling induced shear stress and easily transform martensitically into the monoclinic phase. A linear relationship between applied compressive stress and the degree of tetragonal to monoclinic (t → m) phase transformation was observed. Ball-milling induced microscale stress has a similar effect on the t → m phase transformation. Furthermore, it was found that even very mild milling condition, such as 120 rpm, 1 h (0.5 mm balls) was enough to induce phase transformation. Surfactant assisted ball-milling was found to be very effective in de-agglomeration of our nanocrystalline porous ZrO_2 particles into discrete nanocrystals. However, the t → m phase transformation could not be avoided totally even at very mild milling condition. This suggests that the metastable t-ZrO_2 is extreme sensitive to microscale shear stress induced by both mechanical compression and ball-milling. The findings presented in this work are very important in further understanding the stress-induced phase transformation of nanocrystalline t-ZrO_2 powders in a water free atmosphere and their further stabilization in industrially relevant solvents.

Keywords: ZrO_2; Phase transformation; Milling; Biomedical application; Composites

1. Introduction

Zirconia (ZrO_2) ceramics have found broad applications in energy,[1] catalysis,[2,3] catalysis support,[4] composites[5,6] coatings,[7–9] dental and body implants,[10–14] and solid electrolytes,[15] because of their unusual combination of strength, fracture toughness, ionic and thermal conductivity. These attractive characteristics are largely associated with the stabilization of the tetragonal and cubic phases through alloying with aliovalent ions.

At room temperature (RT) and atmospheric pressure, the thermodynamic stable phase of pure zirconia is the monoclinic and it goes through the following crystal phase as the temperature is raised:

monoclinic → tetragonal → cubic → melt

By suitable control of the processing parameters, however, it is possible to create ZrO_2 in a metastable tetragonal phase at room temperature.[16] The metastable tetragonal phase easily transforms to the monoclinic phase. As a result of the t → m phase transformation, the density of the zirconia crystals is decreased since the crystals expand 3–5 vol%. This volume increase, caused by the martensitic phase transformation, is an important property of t-ZrO_2 (tetragonal zirconia) as it is the basis for transformation toughening, which is used in various applications, e.g. dental inlays, dental crowns and dental bridges where high tensile strength is important.[17]

* Corresponding author. Tel.: +46 10 516 6059.
E-mail address: anwar.ahniyaz@yki.se (A. Ahniyaz).

0955-2219/$ – see front matter © 2010 Elsevier Ltd. All rights reserved.
doi:10.1016/j.jeurceramsoc.2010.05.025

In the last few decades, numerous efforts have been made to understand the phase transformation behaviour of doped zirconia. Effect of particle size, water, and oxygen vacancies on phase transformation of YSZ has been reported.[18,19]

Effect of uniaxial stress on tetragonal to monoclinic (t-m) phase transformation has been reported.[20]

There are only a few reports on the effect of external mechanical stress on the phase transformation behaviour of undoped ZrO_2.

The most often described phase transformation is from monoclinic to tetragonal[21–23] as well as the direct transformation from monoclinic to cubic is seen,[24] but also the reverse reaction (tetragonal to monoclinic) is reported.[25] These varying and contradicting results can be expected to be an effect of different milling conditions (e.g. wet or dry milling) and the history of the zirconia. Regarding the stabilizing effect of ball-milling on the tetragonal and the cubic phase at room temperature several theories have been proposed: lattice imperfections caused by quenching on high-energy impact,[24] incorporations of impurities due to wearing of the milling media,[21,22] and small crystallite size have been suggested.[26]

Unfortunately, however, in most cases, ball-milling experiments were done in uncontrolled atmosphere, like open air, where phase transformation may occur also under the influence of water vapor, for example. Therefore, it is very difficult to evaluate the effect of milling and stress on the phase stability of zirconia crystals and this leads to different conclusions. Moreover, all these previous studies were limited on doped-zirconia, such as yttria-stabilized zirconia (YSZ) and ceria-stabilized zirconia (CSZ).[27–29]

To our knowledge, effect of microscale shear stress on the martensitic phase transformation of nanocrystalline t-ZrO_2 has never been reported.

It is well known that yttria-stabilized zirconia (YSZ) particles embedded in a ceramic matrix can display autocatalysis. That is, the t → m phase transition of one particle induces a strain field in the surrounding matrix that triggers the phase transition in neighbour particles.[30]

The behaviour of YSZ powder alone is anticipated to be very different from that of YSZ particles in a ceramic matrix. In the latter case, the ceramic matrix encloses the YSZ particles and acts as an elastic medium that transfers stresses between YSZ particles that are not in direct contact. In contrast, for YSZ powder, stress transfer can only occur by direct particle-to-particle contact. This implies that the microscale stress state differs from the macroscale stress state. As an example, consider powder subjected to macroscopic compression in a rigid die (Fig. 1). At the macroscale, the YSZ powder is subjected to uniaxial strain. However, at the microscale, individual particles touch each other and transfer stresses via the contact points. Then, at the microscale, the particles are subjected to a complicated stress state involving compressive, shear and possibly also tensile stresses. The presence of shear stresses at the microscale can induce the t → m phase transition in some crystal in some of the YSZ particles. The transforming crystals may bring on autocatalytic phase transition in the crystals they are bonded to. The similar autocatalytic behaviour can be expected for undoped

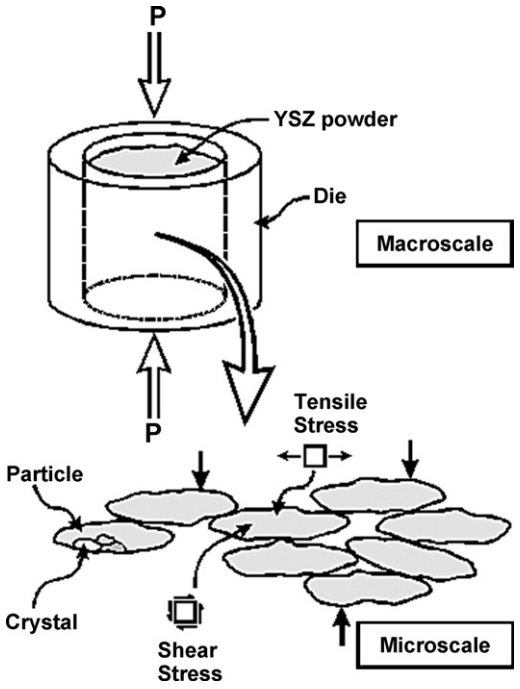

Fig. 1. A schematic illustration showing how particle-to-particle contact can generate microscale shear stresses and tensile stresses although the macroscopic applied stress in compression.

t-ZrO_2. The hypothesis is that a macroscopic compression stress may cause a t → m phase transition in t-ZrO_2 powders due to microscale shear stresses. If true, this hypothesis has the important implications on the ways that pure t-ZrO_2 powder should be handled, since any mechanical treatment of t-ZrO_2 powder will generate microscale stresses that can induce the t → m phase transition.

In the present work, the effect of microscale shear stress originating at particle scale during uniaxial strain test and low speed ball-milling on the crystal phase of zirconia are investigated in carefully controlled atmosphere with XRD, transmission electron microscopy (TEM) and photo correlation spectroscopy. Special attention was paid to avoid any possible water contact with the zirconia samples to evaluate the effect of shear stress on the stability of t-ZrO_2.

2. Experimental methods

All chemicals were supplied by Aldrich and they were all used as received. Highly porous nanocrystalline tetragonal zirconia powders were synthesized by controlled hydrolysis of $ZrOCl_2$ followed by careful calcination.[31] The t-ZrO_2 powders are extremely porous and have specific surface area of ∼150 m^2/g. The powder is very sensitive to water vapor and a few seconds air exposure is enough to cause martensitic phase transformation from tetragonal to monoclinic phase. Therefore synthesized t-ZrO_2 powders were kept in water free environment for further treatment.

2.1. Uniaxial strain testing

In inert atmosphere in a glove box, 200 mg zirconia was placed in pressing tools with a diameter of 13 mm. The press was sealed from atmosphere with nitrile rubber to prevent phase transformation due to reaction of zirconia with water vapor in the air.[32] The samples were exposed to macroscopic compression to pressures of 60, 120 or 188 MPa. The pressure was applied with a speed of 2 kN/min until the maximum value reached and thereafter the pressure was decreased linearly with time back to zero. Data for time, piston position and load was collected at a PC at a data acquisition rate of 10 Hz.

After releasing the pressure, the samples were carefully transferred back to the glove box and mixed with a methacrylic monomer mixture consisting of Bisphenol-A diglycidyl ether dimethacrylate (Bis-GMA), urethane dimethacrylate (UDMA) and triethylene glycol dimethacrylate (TEGDMA) in the ratio (36/44/20 wt%) in combination with a polymerization system composed of champhorquinone and ethyl 4-dimethylamino benzoate both in contents of 0.5 wt% of resin. A sample of this was placed between two glass plates and cured for 2 min using blue light (1100 mW) from a Bluephase® light source (Ivoclar Vivadent, Lichtenstein). This treatment was done as the polymer matrix prevents the tetragonal crystals to undergo phase transformation. The cured samples were then subjected directly to the XRD measurement for the phase analysis.

2.2. Ball-milling

A 250 ml Si_3N_4 coated stainless steel grinding bowl was filled with 60 g of aggregated t-zirconia nanocrystals in anhydrous isopropanol (35 wt%), ~12 g of either polyethylene hexamine or a 1:1 mixture of urethane dimethacrylate:triethylene glycol dimethacrylate and ~150 g of 0.5 mm $ZrSiO_4$ in Ar atmosphere in the glove box and after sealed carefully with tape. The 0.5 mm zircon balls ($ZrSiO_4$) used in our milling experiment were kindly provided by Comballs Corp., Graphtech Materials Co. Ltd., Qing Dao, China. The zirconia powder was milled with Fritsch P6 planetary monomill at 120, 250 or 500 rpm. Samples of the milled dispersion were collected after 1, 3 and 18 h. After milling, the zirconia dispersions were moved into pre-dried anhydrous isopropanol. It was transferred into the glass bottles; the $ZrSiO_4$ balls remained in the grinding bowl. The milled zirconia samples were dried under vacuum and mixed, in the glove box, with a methacrylic monomer mixture consisting of Bisphenol-A diglycidyl ether dimethacrylate (Bis-GMA), urethane dimethacrylate (UDMA) and triethylene glycol dimethacrylate (TEGDMA) in the ratio (36/44/20 wt%) in combination with a polymerization system composed of champhorquinone and ethyl 4-dimethylamino benzoate both in contents of 0.5 wt% of resin. A sample of this was placed between two glass plates and cured for 2 min using blue light (1100 mW) from a Bluephase® (Ivoclar Vivadent, Lichtenstein). The samples were subjected directly to the XRD measurement for the phase analysis.

2.3. Characterization

2.3.1. X-ray diffraction (XRD)

XRD patterns were scanned in 0.1 steps (2θ), in the 2θ range from 26.5° to 33°, with a fixed counting time (40 s). The XRD patterns were analyzed using WinX^{POW} software (STOE & Cie GmbH, Darmstadt, Germany). The obtained values of the t-ZrO_2 and m-ZrO_2 volume fractions (v_t and v_m) were compared with the values obtained from the integral intensities of the monoclinic diffraction lines (−1 1 1) and (1 1 1) and the tetragonal diffraction line (1 0 1), following a procedure proposed by Toraya et al.[33]

2.3.2. Transmission electron microscopy (TEM)

Low- and high-resolution TEM images and Selected Area Electron Diffraction (SAED) patterns were obtained using a JEOL JEM-3010 microscope operating at 300 kV (Cs = 0.6 mm, point resolution 0.17 nm). Images were recorded with a CCD camera (MultiScan model 794, Gatan, 1024 μm × 1024 μm) at a magnification of 4000–400,000 times. TEM samples were prepared by applying a drop of zirconia–isopropanol dispersion onto a carbon coated Cu grid and the solvent was allowed to slowly evaporate at room temperature.

2.3.3. Photon correlation spectroscopy

Particle size distribution was analyzed using a Zetasizer (Nano ZS, 2003, Malvern Instruments, UK). Refractive indices for isopropanol and zirconia were set at 1.39 and 2.2, respectively. Viscosity of the solvent at 25 °C was set to 2.32×10^{-3} Pa s. The standard general-purpose algorithm was the default for the analysis.

All mixing was done by shaking and measurement was carried out immediately after mixing. The sample bottle was thoroughly shaken by hand for 10 s before diluting it with isopropanol and the diluted sample was analyzed by size measurement. This procedure was chosen to be able to measure the overall size distribution of the samples.

3. Results

3.1. Uniaxial strain test

Recorded XRD patterns of the casted ZrO_2 samples from the uniaxial strain test are shown in Fig. 2. For the sample exposed to 60 MPa the (1 0 1) reflection at 30.2° (2θ) is dominating, but as the applied pressure increases, the reflection from the tetragonal zirconia diminishes and the two reflections at 28.2° and 31.4° (−1 1 1 and 1 1 1) from monoclinic zirconia grow in intensity. It can be seen in Fig. 2 that an increased applied compressive stress increases the monoclinic volume fraction in the sample.

In Fig. 3, the volume fraction of phase-transformed crystals are plotted against the maximum applied pressure. The figure shows that the volume fraction increases approximately linearly with the maximum pressure.

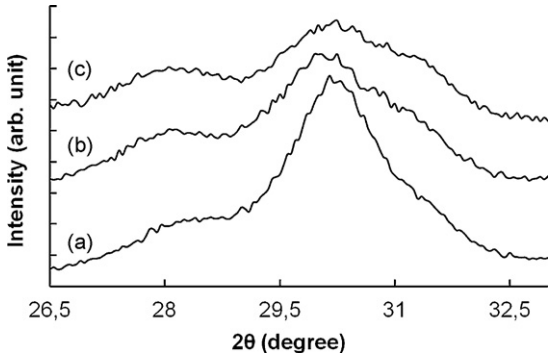

Fig. 2. XRD of zirconia after one axial strain test at different applied pressures, (a) 60 MPa, (b) 120 MPa and (c) 188 MPa.

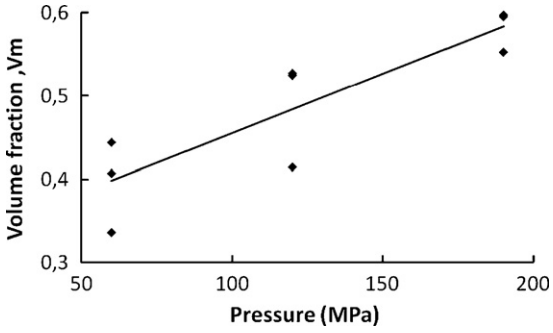

Fig. 3. Volume fraction of formed monoclinic zirconia as a function of applied pressure.

3.2. Ball-milling

The XRD patterns recorded from the milled and in casted samples at different milling speed after 1 and 18 h are illustrated in Figs. 4 and 5. For both experiments, the reflection (1 0 1) of tetragonal zirconia at $30.2^\circ = 2\theta$ dominates after 1 h milling. The two reflections (-1 1 1 and 1 1 1) from monoclinic zirconia grow during milling and the (1 0 1) reflection decreased, indicating a tetragonal to monoclinic transformation.[33] It is also seen that when milling speed is increased to 500 rpm, transformation rate is also significantly higher than 250 rpm.

Phase transformation of the zirconia crystals caused by milling is shown in Fig. 6. It can be seen that the monoclinic volume fraction (v_m) increases with elongated milling time and that

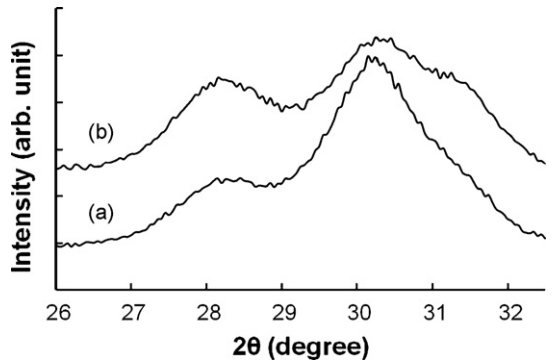

Fig. 4. XRD patterns showing the evolution of m-phase produced by ball-milling of tetragonal zirconia nanoparticles at 120 rpm, (a) 1 h and (b) 18 h.

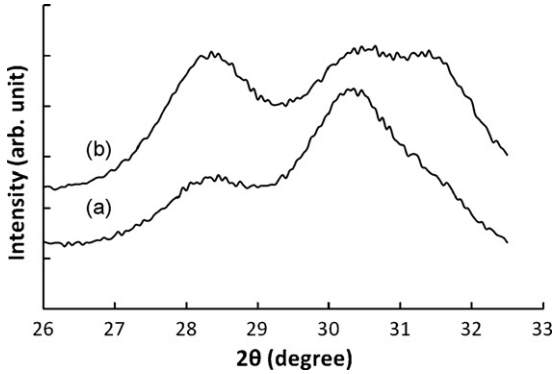

Fig. 5. XRD of zirconia milled (a) 1 h and (b) 18 h at 250 rpm.

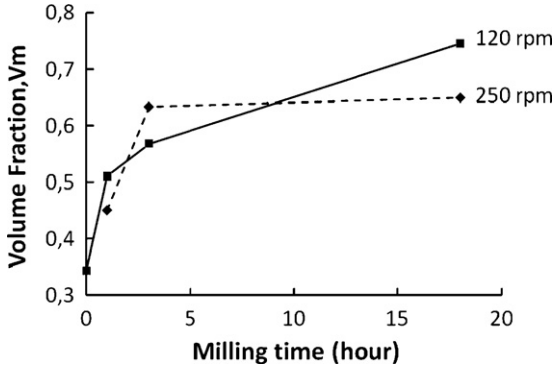

Fig. 6. Volume fraction of formed monoclinic zirconia function a milling time at 120 and 250 rpm.

the results from the 120 and 250 rpm experiments have approximately the same curve progression. As indicated in Fig. 6 the effect of milling speeds at low speed, such as 120 and 250 rpm is not very significant in respect to transformation rate.

Fig. 7 shows the XRD patterns before and after milling. Before milling, the sample mainly consists of tetragonal ZrO_2 giving broad peaks in the XRD patterns as a result of small crystal sizes. The amount of tetragonal phase diminishes as a result of milling but the crystal size remains at 8 nm, calculated by the Scherrer equation:

$$\tau = \frac{K\lambda}{\beta \cos\theta},$$

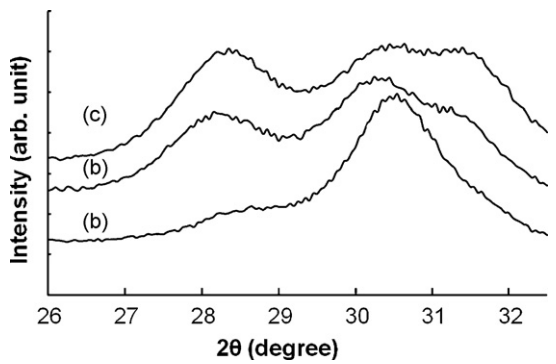

Fig. 7. XRD patterns of zirconia powders before and after milling, (a) before milling, (b) milling at 120 rpm, 18 h and (c) 250 rpm, 18 h.

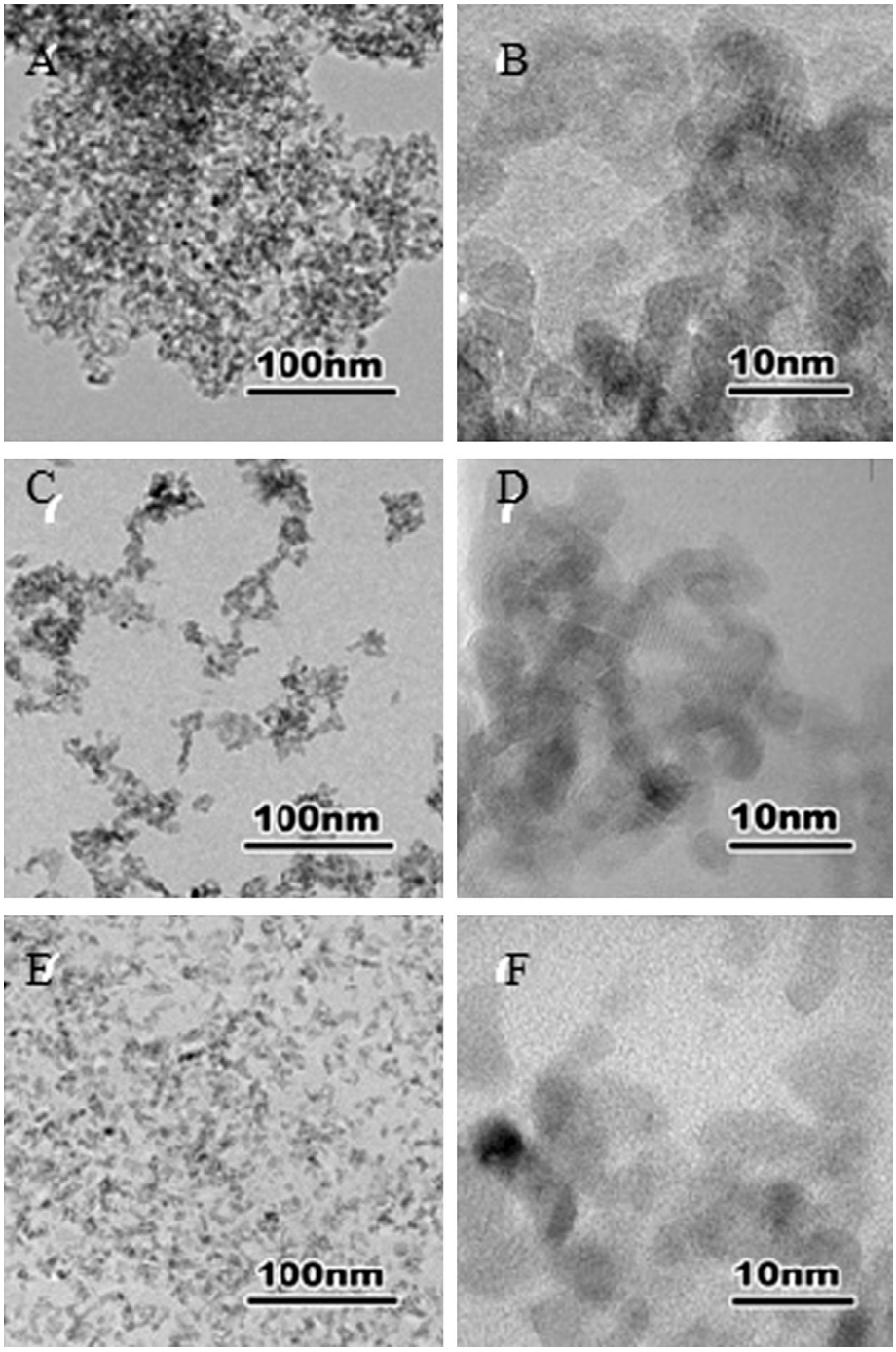

Fig. 8. TEM images of the zirconia particles milled with 0.5 mm $ZrSiO_4$ balls: (A and B) prior to milling; (C and D) milled at 500 rpm, 4 h (E and F) 500 rpm, 18 h.

where τ is the mean crystallite dimension, K is the shape factor, λ is the X-ray wavelength (1.54 Å for Cu K_α), β is the full widths at half maximum intensity (FWHM) in radians, and θ is the Bragg angle. The dimensionless shape factor varies with the shape of the crystallite, but has typically a value about 0.9.[34]

It was confirmed by the transmission electron microscope analysis (Fig. 8a and b) that as prepared samples indeed composed of very small, about 8–10 nm size nanocrystals which are interconnected and makes three dimensional porous networks with an average particle size of about 2.0 μm.

The average size of the milled ZrO_2 particles was determined using photo correlation spectroscopy. The results from the milling experiment performed at a speed of 120 rpm are shown in Fig. 9. The size distribution of milled ZrO_2 that was obtained from DSL analysis agrees well with the result obtained by TEM analysis. For both milling speeds, the particle size reaches a minimum at which point further milling only will give more phase transformation and not lead to further de-agglomeration. Although it is not possible to reduce the average size of milled ZrO_2 particles to less than approximately 300 nm with speed

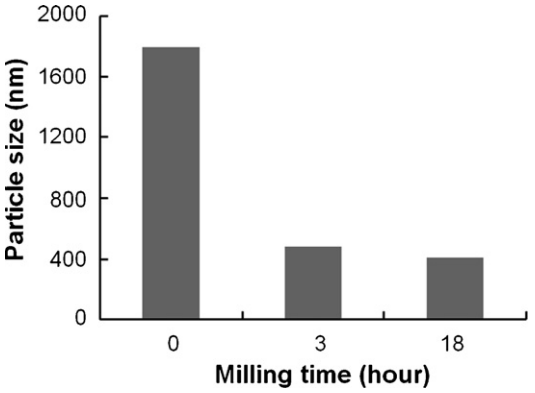

Fig. 9. Size distribution of zirconia particles milled at 120 rpm that is dispersed in isopropanol obtained by dynamic light scattering analysis.

milling such as 120 rpm or 250 rpm, it is interesting, however, to observe the possibility of reducing the particle size to less than 100 nm by prolonged milling of the powders together with suitable surfactants at 500 rpm (Fig. 8). TEM result (Fig. 8e and f) showed that by high energetic ball-milling it is possible to break down the porous network of the zirconia particles and de-aggregate them almost to their primary crystals.

4. Discussion

During the experimental work with the high surface area zirconia powder it became clear that the nanocrystalline t-ZrO_2 is very sensitive towards shear stress. In the compression tests we found phase transformation; this may result from the multi-axial stress field at micro/nanoscale. Likewise, milling test also generates a complicated microscale stress field that induces zirconia undergo a martensitic phase transformation. The increase in the monoclinic volume fraction with increasing applied maximum pressure could be due to an increase in the microscale shear stresses causing enhanced transformation. It is remarkable to observe the similar phase transformation can occur even with our undoped t-ZrO_2.

Furthermore, in the uniaxial strain tests, we have observed a correlation between $t \rightarrow m$ phase transformation rate and specific surface area. Higher the surface area, faster the transformations is. This observation makes us believe that $t \rightarrow m$ phase transformation must be caused by the structural rearrangement of atoms to compensate the accumulated stress at the outermost surface of the t-ZrO_2 nanocrystals, which is further enhanced by the additional shear stress that is provided to the system with extra energy to overcome the activation energy for phase transformation. The porous t-ZrO_2 powders are formed from interconnected nanocrystals. Transforming nanocrystals at the surface may bring autocatalytic phase transformation in the neighbour nanocrystals that they bound to. Although it is impossible for us to determine the defect concentration of the nanocrystalline ZrO_2 powder, it is most likely that the high surface area of our zirconia powders can be correlated to an increased defect concentration on the surface compared with the surface defect concentration of low surface area t-ZrO_2 powders and we assume that the tested zirconia powder, with a high surface area will have more defects per gram, than the low surface area t-ZrO_2. Therefore, we have a reason to believe that $t \rightarrow m$ phase transformation must follow the similar reaction pathway that was reported for doped zirconia.[20,32]

The observed phase transformation in the milling experiments, probably also caused by the complicated stress field, which will cause some shear stresses and shear strains resulting in the phase transformation, just as in the uniaxial strain tests. It is also seen from the XRD patterns that this transformation is little more pronounced in the sample milled at 250 rpm (Figs. 5 and 6). This makes sense as the produced shear stresses depend on the energy supplied to the system. Higher speed will probably cause higher stresses causing an increasing transformation rate. That the difference between the two transformation rates is not more pronounced could be due to the fact that at these relatively low rpm's the balls are still circling at the bottom of the grinding bowl. As shown in Fig. 6 the transformation rate ($t \rightarrow m$) increases with the increasing milling time, but seems to approach a maximum value. This indicates that milling alone will not cause 100% phase transformation, at least not at these low milling speeds.

In comparison with t-zirconia powders which have relatively low surface area, the nanocrystalline zirconia powder that was obtained with our method[31] possesses very high surface area (150 m^2/g). But even though the zirconia powder is very porous (Fig. 8a and b) and milling makes the zirconia change from tetragonal to monoclinic phase. Indeed, mild milling condition, such as 250 rpm, is not strong enough to separate other than loosely agglomerated particles. However, it is possible to break up these interconnected nanocrystals under more energetic milling conditions, such as 500 rpm or higher. This must be due the fact that the zirconia crystals are sintered during the calcinations and apparently milling at low speed does not give enough force to break the sintered crystals from each other.

5. Conclusion

Low milling speed can induce the martensitic phase transformation from tetragonal to monoclinic crystal phase of nanocrystalline zirconia powders. Likewise, macroscopic compression was found to generate the $t \rightarrow m$ phase transition of zirconia powders. At the microscale, both tests induce shear stress in the nanocrystalline zirconia particles. It is proposed that the phase transition caused by milling and compression of zirconia powders induces microscale shear stresses that are responsible for phase transformation.

The present study provides an improved understanding to the phase transformation behaviour of undoped t-ZrO_2 powders under shear stress that was induced by uniaxial compression and ball-milling.

Acknowledgements

This work was financially supported by the DentoFit A/S. We thank Mads Gudik-Sørensen for assistance with powder XRD.

Appendix A. Supplementary data

Supplementary data associated with this article can be found, in the online version, at doi:10.1016/j.jeurceramsoc.2010.05.025.

References

1. Adler SB. Factors governing oxygen reduction in solid oxide fuel cell cathodes. *Chem Rev* 2004;**104**(10):4791–843.
2. Reddy BM, Patil MK. Organic syntheses and transformations catalyzed by sulfated zirconia. *Chem Rev* 2009;**109**(6):2185–208.
3. Korotcenkov G, Do Han S, Stetter JR. Review of electrochemical hydrogen sensors. *Chem Rev* 2009;**109**(3):1402–33.
4. Wang CM, Fan KN, Liu ZP. Origin of oxide sensitivity in gold-based catalysts: a first principle study of CO oxidation over Au supported on monoclinic and tetragonal ZrO_2. *J Am Chem Soc* 2007;**129**(9):2642–7.
5. Otsuka T, Chujo Y. Poly(methyl methacrylate) (PMMA)-based hybrid materials with reactive zirconium oxide nanocrystals. *Polym J* 2000;**42**(1):58–65.
6. Garnweitner G, Goldenberg LM, Sakhno OV, Antonietti M, Niederberger M, Stumpe J. Large-scale synthesis of organophilic zirconia nanoparticles and their application in organic–inorganic nanocomposites for efficient volume holography. *Small* 2007;**3**(9):1626–32.
7. Golosnoy IO, Cipitria A, Clyne tW. Heat transfer through plasma-sprayed thermal barrier coatings in gas turbines: a review of recent work. *J Therm Spray Technol* 2009;**18**(5–6):809–21.
8. Schulz U, Leyens C, Fritscher K, Peters M, Saruhan-Brings B, Lavigne O, et al. Some recent trends in research and technology of advanced thermal barrier coatings. *Aerospace Sci Technol* 2003;**7**(1):73–80.
9. Zhong XH, Wang YM, Xu ZH, Zhang YF, Zhang JF, Cao XQ. Hot-corrosion behaviors of overlay-clad yttria-stabilized zirconia coatings in contact with vanadate-sulfate salts. *J Eur Ceram Soc* 2010;**30**(6):1401–8.
10. Denry I, Kelly JR. State of the art of zirconia for dental applications. *Dent Mater* 2008;**24**(3):299–307.
11. Zinelis S, Thomas A, Syres K, Silikas N, Eliades G. Surface characterization of zirconia dental implants. *Dent Mater* 2010;**26**(4):295–305.
12. Nagarajan S, Rajendran N. Sol–gel derived porous zirconium dioxide coated on 316L SS for orthopedic applications. *J Sol–Gel Sci Technol* 2009;**52**(2):188–96.
13. Hisbergues M, Vendeville S, Vendeville P. Zirconia-established facts and perspectives for a biomaterial in dental implantology. *J Biomed Mater Res B* 2009;**88B**(2):519–29.
14. Chevalier J, Gremillard L, Deville S. Low-temperature degradation of zirconia and implications for biomedical implants. *Ann Rev Mater Res* 2007;**37**:1–32.
15. Shim JH, Chao CC, Huang H, Prinz FB. Atomic layer deposition of yttria-stabilized zirconia for solid oxide fuel cells. *Chem Mater* 2007;**19**(15):3850–4.
16. Becker J, Hald P, Bremholm M, Pedersen JS, Chevallier J, Iversen SB, et al. Critical size of crystalline ZrO_2 nanoparticles synthesized in near- and supercritical water and supercritical isopropyl alcohol. *ACS Nano* 2008;**2**(5):1058–68.
17. Ardlin BI. Transformation-toughened zirconia for dental inlays, crowns and bridges: chemical stability and effect of low-temperature aging on flexural strength and surface structure. *Dent Mater* 2002;**18**(8):590–5.
18. Chevalier J, Gremillard L, Virkar AV, Clarke DR. The tetragonal–monoclinic transformation in zirconia: lessons learned and future trends. *J Am Ceram Soc* 2009;**92**(9):1901–20.
19. Jimenez S, Carmona S, Castano VM. Zirconia nanoparticles: a martensitic phase transition at low temperature. *J Exp Nanosci* 2009;**4**(1):95–103.
20. Subhash G, Nemat-Nasser S. Uniaxial stress behaviour of Y-TZP. *J Mater Sci* 1993;**28**(21):5949–52.
21. Stefanic G, Music S, Gajovic A. Structural and microstructural changes in monoclinic ZrO_2 during the ball-milling with stainless steel assembly. *Mater Res Bull* 2006;**41**(4):764–77.
22. Gajovic A, Furic K, Stefanic G, Music S. In situ high temperature study of ZrO_2 ball-milled to nanometer sizes. *J Mol Struct* 2005;**744**:127–33.
23. Stefanic G, Music S, Gajovic A. A comparative study of the influence of milling media on the structural and microstructural changes in monoclinic ZrO_2. *J Eur Ceram Soc* 2007;**27**(2–3):1001–16.
24. Bid S, Pradhan SK. Preparation and microstructure characterization of ball-milled ZrO_2 powder by the Rietveld method: monoclinic to cubic phase transformation without any additive. *J Appl Crystallogr* 2002;**35**:517–25.
25. Adam J, Drumm R, Klein G, Veith M. Milling of zirconia nanoparticles in a stirred media mill. *J Am Ceram Soc* 2008;**91**(9):2836–43.
26. Kuznetsov PN, Kuznetsova LI, Zhyzhaev AM, Kovalchuk VI, Sannikov AL, Boldyrev VV. Investigation of mechanically stimulated solid phase polymorphic transition of zirconia. *Appl Catal A* 2006;**298**:254–60.
27. Matsuzawa M, Abe M, Horibe S. Strain rate dependence of tensile behavior and environmental effect in zirconia ceramics. *ISIJ Int* 2003;**43**(4):555–63.
28. Sun QP, Zhao ZJ, Chen WZ, Qing XL, Xu XJ, Dai FL. Experimental-study of stress-induced localized transformation plastic zones in tetragonal zirconia polycrystalline ceramics. *J Am Ceram Soc* 1994;**77**(5):1352–6.
29. Rauchs G, Fett T, Munz D, Oberacker R. Tetragonal-to-mono clinic phase transformation in CeO_2-stabilised zirconia under uniaxial loading. *J Eur Ceram Soc* 2001;**21**(12):2229–41.
30. Stump DM. Autocatalysis-the self-induced growth of martensitic phase-transformations in ceramics. *Acta Metall Mater* 1994;**42**(9):3027–33.

[31]. Van Lelieveld A, Almdal K, Linderoth S, Sørensen BF. WO2005099652-A1 (2005).

32. Guo X. Property degradation of tetragonal zirconia induced by low-temperature defect reaction with water molecules. *Chem Mater* 2004;**16**(21):3988–94.
33. Toraya H, Yoshimura M, Somiya S. Calibration curve for quantitative-analysis of the monoclinic–tetragonal ZrO_2 system by X-ray-diffraction. *J Am Ceram Soc* 1984;**67**(6):C119–21.
34. Smilgies DM. Scherrer grain-size analysis adapted to grazing-incidence scattering with area detectors. *J Appl Crystallogr* 2009;**42**(6):1030–4.